RSC Advances

ROYAL SOCIETY OF CHEMISTRY

www.rsc.org/advances

Electrochemical Properties of Ce (III) in Equimolar Mixture of LiCl-KCl and NaCl-KCl Molten Salts

[1,3]D. K. Sahoo,[2,3]A. K. Satpati* and [3]N. Krishnamurthy
[1]Rare Earths Development Section,[2]Analytical Chemistry Division
Bhabha Atomic Research Centre, Trombay, Mumbai-400 085
[3]Homi Bhabha National Institute, Mumbai-400 094

Abstract:

Electrochemical behavior of $CeCl_3$ was investigated in two molten chloride mixtures, equimolar LiCl-KCl and NaCl-KCl melts using inert molybdenum and tungsten electrodes in the temperature range of 963 to 1053 K. Electrochemical methodologies like, cyclic voltammetry and square wave voltammetry were employed to investigate the electrode process. Results showed that reduction of Ce (III) to Ce (0) is quasireversible to irreversible in nature in both of these melts. Diffusion coefficient of Ce (III) was determined in both the systems at four different temperatures and Arrhenius treatment was employed to obtain the activation energy for the diffusion process in the molten salt mixtures. The exchange current density of Ce(III)/Ce(0) was evaluated in both the melts on Mo and W electrodes at four different temperatures from the Tafel plot.

Key words: Cerium electrochemistry, Molten salts, Cerium chloride, Diffusion coefficient, Exchange current density.

==

***Corresponding Author**
Dr. A. K. Satpati
Bhabha Atomic Research Centre
Trombay, Mumbai-400 085
Tel-91-2225590326
Fax-91-2225505151
Email: aksatpati@gmail.com

1. **Introduction**

Rare earths are extremely important materials in numerous green technologies on account of their unique combination of chemical, electronic, magnetic and optical properties [1-3]. Apart from separation of the naturally occurring rare earths from one another in the head-end processing operations, preparation of pure elemental form of individual rare earths is considered as an important and technologically challenging process. The processes involved are metallothermic reduction of rare earth halides or oxides and fused salt electrolysis in a chloride or oxide-fluoride media. Fused chloride electrolysis for making rare earth metals is attractive because of low cost, ease of operation, batch size and purity of the product. The process is particularly attractive for the synthesis of light rare earth metals and alloys [4-5]. The electrolytes used in such process are mostly rare earth chlorides with mixtures of alkali or alkaline chlorides. The hygroscopic nature of alkaline earth chlorides makes them unfavorable over alkali earth chlorides. LiCl-KCl and NaCl-KCl are the most common solvents used for such purposes [6-8]. The major problem associated with fused chloride electrolysis is the low current efficiency which limits the wide spread and easy implementation of this process. The motivation of this research is to study the kinetic properties of molten salt-electrode reaction which could affect current efficiency in the electro-winning of cerium metal.

Molten salt electrolytic technology has been considered as a good option for the reprocessing of metallic nuclear fuels [9-10]. Among various molten salts, fused alkali halides were found to be the suitable media for this purpose [11-14]. The process involves effective separation of actinides from the lanthanides in the fission products. Hence, determining kinetic parameters related to reduction of lanthanide and actinide ions in molten chloride media are extremely important in the design of advanced electrochemical processors.

Cerium is the most abundant elements among all the 17 rare earths. It is also a typical element in the fission products which is very much similar to uranium. Therefore, it is important to study the electrochemistry of cerium ion in molten chloride medium for the effective use of molten salt electrolysis technology in both metal preparation and reprocessing of nuclear fuels. In the present work, the electrochemical behavior of cerium ion in LiCl-KCl and NaCl-KCl melts has been investigated using molybdenum and tungsten electrodes. Limited published work was found on high temperature electrochemistry investigations of cerium in molten salts. Castrillejo et.al.[15] have studied the electrochemical behavior of cerium in LiCl-KCl melt at 723K. Fusselman et al. [16] and Lantelme et.al. [17] have discussed about the standard potential of cerium reduction in LiCl-KCl between 673-773 K and 650-880 K. Izuka et.al.[18] have measured the diffusion coefficient at the temperature range between 673-873K by chronopotentiometry technique. Reduction of Ce (III) on cerium anode was investigated by Marsden et al. [19]. Recently electrochemical behavior of cerium ion on molybdenum electrode in LiCl-KCl eutectic was investigated by Wang et al. [20] in the temperature range of 673-873 K. Most of these literatures reported the thermodynamic properties compared to kinetic parameters. Moreover, the kinetic data reported by some researchers are not sufficient in the research field due to different experimental conditions like salt composition and material of working electrodes. Apart from that, electrochemical data of the reduction of Ce (III) in NaCl-KCl are rarely found in the literatures, although it is considered as a better media to get the metal ingot. Therefore, Present study was carried out to investigate the electrochemical properties of Ce (III) both in LiCl-KCl and NaCl-KCl melt on inert electrodes (Tungsten and Molybdenum) at higher operational temperatures compared to previous studies to get the inherent mechanism and kinetics of electrochemical process. Higher operational temperature also allowed us to compare the kinetic parameters of the electrochemical process in LiCl-KCl medium with that of NaCl-KCl medium. The aim was to first probe the reaction mechanism and to determine the kinetic parameters like diffusion coefficient and exchange current densities which are important and relevant in the formation of Ce metal by electrochemical deposition from molten salts mixtures. The results may help to do further research in the efficient extraction of rare earth metals by electrolytic reduction process.

2. Experimental

2.1 Chemicals

The starting material used was $CeCl_3$, $7H_2O$ (99.9% pure), Potassium chloride, sodium chloride and lithium chloride having 99.5% purity of LR Grade. These chemicals were procured from SD fine chemicals, Mumbai.

2.2. Preparation and purification of the electrolyte

The salt $CeCl_3.7H_2O$ was dehydrated by step wise heating under dynamic vacuum up to 200°C for 24 hours. The sample was further heated at 200 °C under flowing argon with dry HCl gas to prevent the possible hydrolysis reaction to form CeOCl. The final product was verified for any unwanted CeOCl by HCl dissolution test. All the solvents, LiCl, KCl and NaCl were dehydrated under dynamic vacuum in the temperature range of 373-773 K. Then chloride mixtures i.e. LiCl-KCl (1:1) and NaCl-KCl (1:1) were pre melted in an alumina crucible under an argon atmosphere. Calculated amount of anhydrous $CeCl_3$ was put into the treated LiCl-KCl and NaCl-KCl melts. The LiCl-KCl and NaCl-KCl melts were melted at higher temperature for better mixing and then the mixture was cooled down. This well mixed composition was reheated and melted and the temperature of the melt was raised at the desired experimental temperatures. Then the analyte was added and the mixture was allowed equilibrate at the set temperature. All the experiments were carried out under inert atmosphere by purging high purity argon gas.

The total concentrations of cerium ion in both the prepared salts were measured by inductive coupled plasma-atomic emission spectroscopy (ICP-AES) analysis.

2.3. Electrolytic cell

The electrolytic cell consists of a vacuum tight inconel retort of 70 mm diameter and 500 mm length fitted with a stainless steel flange having ports for inserting the working electrode, counter electrode, reference electrode and the thermocouple. Electrolytic mixture was charged into an alumina crucible which was kept inside the inconel retort. The whole electrochemical cell was placed inside a tubular vertical resistance furnace. The resistance furnace with electronic temperature control unit (accuracy $\pm 2^0$C) was used to heat the cell to the operating temperature. The schematic of the electrolytic setup is shown in Fig.1.

2.4. Instrumentations

A three electrode system was used for the electrochemical measurements. The inert working electrode was prepared using 1 mm metallic molybdenum or tungsten wire. The counter and reference electrodes were made up of tungsten wire of 2 mm and 1 mm diameters respectively. Tungsten was used as quasireference electrode because it is inert and stable in molten salt at high temperature. The surface of the electrodes were polished with emery paper of 1200 grit and then cleaned with acetone. The geometrical surface area of the working electrode was determined by measuring the depth of immersion of the wire into the molten salt. All the electrochemical measurements were recorded using Zahner Electrochemical workstation, Germany equipped with IM6 interface. Cyclic voltammetric experiments were carried out after stabilization of the open circuit potential. Multiple blank scans were recorded to ascertain the stability of the melt. The voltammograms were recorded and analyzed using Thales software package. Energy dispersive X-ray fluorescence (EDXRF) was carried out using EX-3600 M spectrometer from Xenemetrix. Scanning electron microscope (SEM) was carried out using the instrument from Cam scan, UK. The solidified melt was washed repeatedly with hexane prior to SEM and EDXRF measurements.

3. Results and discussion

3.1 Reduction behavior of Ce (III) in LiCl-KCl and NaCl-KCl systems characterized by cyclic voltammetry

Cyclic voltammetry study was carried out to probe the reaction mechanism of electrochemical reduction of Ce^{3+}/Ce**.** The voltammograms obtained at 963 K with 2.1×10^{-4} mol/cm^3 $CeCl_3$ at molybdenum electrode using LiCl-KCl electrolyte are shown in Fig. 2. The dashed curve shows the voltammogram of the blank salt which has no additional peak except the reduction and the corresponding oxidation peak of lithium in the electrochemical window investigated. After the addition of $CeCl_3$, a cathodic peak at -2.0 V and corresponding anodic peak at -1.84 V were observed in the voltammogram. Energy dispersive X-ray Fluorescence Spectra (EDXRF) of the deposited product was carried out to obtain elemental information of the deposited product and the results are shown in Fig.3. These experiments were carried out using the deposits obtained after applying -2.05 V on the working electrode for 10 minutes. Analysis of the electrodeposited products by EDXRF spectra confirmed the formation of cerium metal on electrochemical deposition. This substantiates that the observed cathodic peak at -2.0 V was due to the reduction of cerium ion to metallic Ce. The peak obtained at -1.84 V during the reverse scan was due to the dissolution of cerium metal in the melt. Electrochemical deposition and dissolution of Ce might be through multistep process; however present cyclic voltammetric scans could not resolve all those elementary deposition and dissolution steps. Instead of that a broad voltammetric plot due to the anodic dissolution of Ce was obtained. Cyclic voltammetric measurements were recorded for the reduction of Ce (III) in equimolar NaCl-KCl melt at 963K which is above the melting point of equimolar mixture of NaCl-KCl i.e. 645 ^{0}C and the results are shown in Fig.4. Reduction peak of Ce (III) in this melt was not as sharp as that of LiCl-KCl. Electrochemical process was assumed as the three electron transfer process considering similar results reported earlier [21]. In the case of LiCl-KCl the Ce (III) reduction peak was well separated from the reduction of Li^+ where as the Ce (III) reduction peak was almost merged with the reduction of Na^+ in the case of NaCl-KCl melt. To check the possibility of formation of Ce-Na intermetallics, atomic absorption spectroscopy (AAS) analysis was carried out of the deposited product obtained after potentiostatic electrolysis at -2.1V for 10 minutes in NaCl-KCl flux. Absence of any sodium ruled out the formation of Ce-Na intermetallics. The narrow difference in the Na^+ and Ce^{3+} reduction peaks is due to the small difference in their electrode potentials.

Morphology of the as deposited Ce metal was investigated from SEM measurements and the micrograph is shown in Fig.5. Uniform crystallite size was observed with the average crystallite diameter of 5 μm.

3.2 Kinetics of the electrode process

Cyclic voltammetry was carried out in both the melts at various scan rates in the temperature range of 963K to 1053K to investigate the dependence of peak potential and peak current on polarization rate. Fig.6 represents the voltammogram recorded in molten $CeCl_3$ (2.1×10^{-4} mole/cc) in equimolar LiCl-KCl electrolyte at 963K at different scan rates. The dependency of the observed peak current with the scan rates is shown in Fig.7. The peak currents (I_c) varied linearly with the square root of scan rates ($v^{1/2}$) of the measurements at the scan rated range investigated, which signify the diffusion controlled electrochemical process. Detailed analysis of voltammograms disclosed more about the kinetics of the electrochemical reduction process. From Fig.6 it was observed that the cathodic peak potential (E_{pc}) shifted slightly towards more negative side and anodic potential (E_{pa}) shifted towards positive side with increase in scan rates. Moreover the separation between cathodic and anodic peak potentials ($\Delta E_p = E_{pa} \sim E_{pc}$) was increasing with the scan rates. All these observations indicated that reduction of Ce (III) on molybdenum substrate was an irreversible electrochemical process. The cyclic voltammograms obtained at different scan rates in NaCl-KCl melt and the dependency of the peak current with the scan rates are shown in Fig. 8 and Fig.9 respectively. It was observed that the reduction peak was more cathodically shifted in NaCl-KCl media compared to that in LiCl-

KCl media. In such molten media two phenomena can affect the peak position; (1) the micro viscosity of the media and (2) the ion association effect of the molten salt. Presently we have not made any detailed investigation about these two phenomena however without a detailed investigation it can be inferred that due to both the phenomena the reduction peak of Ce(III) might be shifted towards more negative direction. The micro viscosity in NaCl-KCl molten salt is higher compared to that in LiCl-KCl media which would shift the reduction peak potential towards cathodic direction. The counter ion association around Li^+ would be higher compared to Na^+ due to the high charge to radius ratio of Li^+. This will result in the comparatively weaker binding between the Ce (III) and the counter chloride ions in the case of LiCl-KCl melt than in NaCl-KCl. Therefore due to this ion association effect also the reduction peak potential might be shifted towards negative direction in NaCl-KCl media. It was also observed that the oxidation peak of Na was decreased with increase in the scan rate in the cyclic voltammetry plots (Fig. 8), though the reduction current of Na^+ reduction was increased with increase in the scan rate of the measurements. This decrease in the oxidation peak current was due to the instability of Na deposits over the Mo working electrode surface and the deposits would peel out from the working electrode substrate when deposited at high discharge rates. Tungsten electrode was also used for the measurements and similar results were obtained for which the results are not shown, thus a similar electrochemical process on both tungsten and molybdenum substrates was proposed.

3.3 Calculation of standard rate constant:

It has been a popular practice to apply the Nicholson and Shain treatment to obtain the kinetic parameters from the cyclic voltammetric measurements [22]. Under this approach the kinetics of the exchange of electrons with the electrode substrate was obtained for the species diffusing to the electrode surface without any adsorption. In the present case Nicholson treatment was applied to verify the reversibility of the electrochemical reduction process. The standard rate constant (*Ks*) of electrode reaction is correlated to a function 'Ψ' according to the following relation

$$\Psi = \frac{K_S}{(\pi DnF/RT)^{1/2}} \frac{1}{\nu^{1/2}} \qquad (1)$$

Where K_s is standard rate constant (cm/s), Ψ is a function related to the difference between cathodic and anodic peak potentials (ΔE_p), *n* is the number of electrons involved in the reduction process, '*F*' is the Faraday constant, '*R*' is the universal gas constant (8.314 J $mol^{-1}K^{-1}$), '*T*' is absolute temperature (K), *D* is the diffusion coefficient (cm^2s^{-1}), 'ν' is the potential sweep rate in (Vs^{-1}) and α is the transfer coefficient which was taken as 0.5.

The dependence of ΔE_p on the Ψ function is given in the Nicholson table [23].The value of Ψ in the Nicholson table represents the function for one electron transfer at room temperature (298K) .The normalized Ψ function (Ψ_T) with respect to operating temperature and 3 electron transfer were calculated using following equations [24]

$$\Delta E_P^{298} = 3 \times \Delta E_P^T \left(\frac{298}{T}\right) \qquad (2)$$

$$\Psi_T = \Psi_{298}\sqrt{\frac{T}{298}} \qquad (3)$$

From the normalized Ψ function (Ψ_T) obtained from Eqs. (2) and (3), the values of standard rate constant (K_s) were estimated at various scan rates using Eq. (1). The values of normalized Ψ function (Ψ_T) and standard rate constant (K_s) for charge transfer on molybdenum electrode at various scan rates in both LiCl-KCl and NaCl-KCl melts are presented in Table 1. It was observed that the value of standard rate constant falls in the quasireversible to irreversible range. At higher scan rates, the normalized Ψ_T values fall beyond the Nicholson table and could not be determined. Based on the Matsudo and Ayabe classification, the electrochemical reaction is regarded as quasireversible in the san range of 0.025 to 0.2 V/s if the estimated Ks value are in the range of $10^{-1} > Ks > 10^{-6}$. Considering this classification, Ks values as shown in Table 1, for the electrochemical reduction of Ce (III) falls in the quasireversible region [25].

Presently the values of Ψ_T falls approximately in the range of 0.2 to 0.6 and α is supposed to have influence in the cyclic voltammogram. However, α has strong influence on the shape of the cyclic voltammetric plot. With decrease in α cathodic peak shits catholically and the anodic peak also shifts catholically thus the peak difference remained unaffected [23]. Therefore the influence of α assumed to be negligible in the present case and the reported standard rate constant values indicated the quasireversible to irreversible nature of the electrochemical process. Similar results were also obtained for tungsten electrode. Therefore, it was concluded that electrochemical reduction of Ce (III) to Ce (0) is quasireversible to irreversible in nature on both tungsten and molybdenum electrode in LiCl-KCl and NaCl-KCl melts.

3.4 Square wave voltammetry:

Square wave voltammetric scans were recorded to investigate the deposition and stripping characteristics during Ce deposition and stripping. Results are shown in Fig.10 and Fig. 11 for of 2.2×10^{-4} mole cm^{-3} of $CeCl_3$ in LiCl-KCl and of 2.0×10^{-4} mole cm^{-3} of $CeCl_3$ in NaCl-KCl melts at 963K at 5 kHz respectively. Only a single reduction peak was observed in the potential range studied which indicated that the electro-reduction of cerium is a single step process in both the flux. It can also be observed that both the peaks are somewhat asymmetric in shape which may be due to the nucleation of rare earth metals as described by previous researchers [26]. In this case the nucleation process was marginally slower compared to the stripping process.

3.5 Calculation of diffusion coefficient and verification of compliance to Arrhenius law:

The linear dependence of cathodic peak current with the square root of scan rate was presented in Fig.7 and Fig.9 respectively for LiCl-KCl and NaCl-KCl melts. For diffusion controlled irreversible electrochemical process, the relation between peak current and diffusion coefficient was given by the following relation [20]

$$i_p = 0.4958 \times n \times F^{3/2} \times A \times (RT)^{-1/2} \times D^{1/2} \times C \times v^{1/2} \times (\alpha n)^{1/2} \qquad (4)$$

Where i_p is cathodic peak current *(A)*, *n* is the number of electrons involved in the reduction process which was taken to be 3, '*A*' is active surface area of working electrode (cm^2), $D_{Ce(III)}$ is the diffusion coefficient (cm^2s^{-1}), '*C*' is the bulk concentration of cerium ion ($molcm^{-3}$), and α is the transfer coefficient which was taken as 0.5 other parameters are same as explained in equation 1. Diffusion coefficients values were calculated by applying the relation between the peak current with scan rate as per the above mentioned equation. The values of diffusion coefficients with standard error at are presented in Table.2.

The diffusion coefficients obtained at various temperatures in both the solvents (LiCl-KCl and NaCl-KCl) are plotted with respect to the experimental temperatures and shown in Fig. 12. Diffusion coefficient values were correlated well with the experimental temperatures as suggested by the Arrhenius treatment

3.6 Estimation of activation energy for the diffusion process:

The diffusion co-efficient values were used to calculate activation energy for the diffusion process. Effect of temperature on the diffusion co-efficient obeys the Arrhenius law through the following equation:

$$D = D_0 exp\left(\frac{-E_a}{RT}\right) \qquad (5)$$

Where D (cm^2s^{-1}) is diffusion co-efficient, E_a is the activation energy (kJ/mole).D_0 is the pre-exponential term (cm^2s^{-1}) in the Arrhenius eqn.

The logarithm of eqn. can be represented as follows

$$\log D = logD_0 - \frac{E_a}{RT} \qquad (6)$$

Fig.12 shows the relationship between log D and 1/T and the slope of the lines in were used to calculate the activation energy for diffusion of Ce (III) ions. Empirical relations between diffusion coefficient and temperature as well as estimated activation energy for diffusion of Ce (III) ions in both the molten salt mixtures are presented in Table-3.

The activation energy for diffusion in the case of NaCl-KCl was higher than in LiCl-KCl. This was reflected in the observation of higher diffusion coefficients in LiCl-KCl melt compared to NaCl-KCl melt. This was possibly due to the comparatively higher viscosity of NaCl-KCl melt.

3.7 Exchange current density:

The exchange current density is an important parameter to know the kinetics of electron transfer during electrochemical reaction. Exchange current density is the reflection of rate of reaction at the equilibrium potential. Here the exchange current density was determined employing the Tafel treatment as shown in Fig.13 and Fig. 14 in two metals. Linear sweep experiments were carried out at a scan rate of 20 mV/s at the potential range of -2.10 V to -1.85 V. Tafel treatment was applied and the exchange current density was calculated and the values of exchange current densities at various temperatures on both molybdenum and tungsten electrodes are given in Table.4. As per the Butler-Volmer equation the Tafel region falls at the moderately higher over potentials. In the present case (cf. Fig. 13 and Fig 14) in the anodic region the diffusion limiting condition started early and there is limited scope of getting the extended linear Tafel region. In the cathodic region there are some more quasi linear regions. However we choose a similar potential difference away from the equilibrium potential. The value of transfer coefficient (α) was also determined from the cathodic slope of Tafel plot.

The exchange current densities as reported previously [19] were in the range of 0.04 to 0.1 Acm^{-2} at 773K.In the present investigation, the exchange current densities were obtained in the range of 0.05 to 0.08Acm^{-2} in the experimental temperature of 963 to 1053K.Thus the current densities at higher experimental temperatures in the present case were lower in comparison to previously reported values [19].A lower value of exchange current density has been reported in the case of La deposition and explained to be due to the lattice mismatch effect between substrate and the deposits [27]. This discrepancy could also be due to the different in melt composition used in the present case i.e.equimolar LiCl-KCl compared to earlier works where exact eutectic composition of LiCl-KCl was taken. However a generalized conclusion on the lowering of exchange current density could not be obtained based on the present findings and the previous reports.

4. Conclusion:

The electrochemical property of $CeCl_3$ in two molten chloride mixtures, LiCl-KCl and NaCl-KCl were studied in the temperature range from 963K to 1053K. The electrochemical reduction showed irreversible behavior according to Nicholson treatments. Diffusion coefficients obtained from different temperatures were found to obey the Arrhenius equation in both the melts. The activation energies for diffusion of Ce (III) ions in both the metals were obtained from the Arrhenius treatment of the correlation of diffusion coefficients with temperatures. The exchange current density values of Ce (III)/Ce (0) were estimated from the Tafel plots generated at four different temperatures in the range of 963 to 1053K. The exchange current density values were in between 0.05 to 0.08 Acm^{-2}. Present results were discussed comparing the previously reported literatures.

References

[1] Y.H. Zhang, T.J. Zhu, J.P. Tu, X.B. Zhao, *Mater. Chem. Phys*., 2007, **103**,484.

[2] A. Sarkis, E. Callen, *Physical Review B*, 1982, **26**, 3870.

[3] F. Soto, L. Cabo, J. Mosqueira, M.V. Ramallo, J.A. Veira, F. Vidal, *EPL (Europhysics Letters),* 2006, **73,** 587.

[4] S. Singh, A.L. Pappachan, *Bull. Mater. Sci*., 1980, **2,** 155.

[5] C.K. Gupta, N. Krishnamurthy, *Int. Mater. Rev*., 1992, **37**,197.

[6] S. Singh, A.L. Pappachan, H.S. Gadiyar, *Journal of the Less Common Metals*, 1986, **120**,307.

[7] L. Feng, C. Guo, D. Tang, *J. Alloys Compd*., 1996, **234**,183.

[8] D. Sahoo, H. Singh, N. Krishnamurthy, *Rare Met*., 2013, **32**, 305.

[9] T. Koyama, M. Iizuka, Y. Shoji, R. Fujita, H. Tanaka, T. Kobayashi, M. Tokiwai*, J. Nucl. Sci. Technol*., 1997, **34**, 384.

[10] K. Kinoshita, T. Inoue, S.P. Fusselman, D.L. Grimmett, J.J. Roy, R.L. Gay, C.L. Krueger, C.R. Nabelek, T.S. Storvick, *J. Nucl. Sci. Technol*., 1999, **36**, 189.

[11] P. Masset, R.J.M. Konings, R. Malmbeck, J. Serp, J.-P. Glatz, *J. Nucl. Mater*.,2005, **344**, 173.

[12] B. Prabhakara Reddy, S. Vandarkuzhali, T. Subramanian, P. Venkatesh, *Electrochim. Acta,* 2004, **49**, 2471.

[13] M. Iizuka, K. Uozumi, T. Inoue, T. Iwai, O. Shirai, Y. Arai, *J. Nucl. Mater*., 2001, **299**,32.

[14] D. Lambertin, J. Lacquement, S. Sanchez, G.S. Picard*, Electrochem. Commun*., 2001, **3** 519.

[15] Y. Castrillejo, M.R. Bermejo, R. Pardo, A.M. Martínez, *J. Electroanal. Chem*., 2002, **522**, 124.

[16] S.P. Fusselman, J.J. Roy, D.L. Grimmett, L.F. Grantham, C.L. Krueger, C.R. Nabelek, T.S. Storvick, T. Inoue, T. Hijikata, K. Kinoshita, Y. Sakamura, K. Uozumi, T. Kawai, N. Takahashi, *J. Electrochem. Soc*., 1999, **146**, 2573.

[17] F. Lantelme, T. Cartailler, Y. Berghoute, M. Hamdani, *J. Electrochem. Soc*., 2001, **148**, C604.

[18] M. Iizuka, *J. Electrochem. Soc*., 1998, **145**, 84.

[19] K.C. Marsden, B. Pesic*, J. Electrochem. Soc*., 2011, **158,** F111.

[20] C. Wang, Y. Liu, H. Hi, F. Gao, L. Liu, S. Chang, J. Guo, L. Chang, Y. Ouyang, *Journal of Rare Earths*, 2013, **31**, 405.

[21] Kh.B.Kushkhov,M.K.Vindizheva and R.A.Karashaeva, *Russian Journal of Electrochem*., 2006, **42**, 830.

[22] R. S. Nicholson, I. Shain, *Anal. Chem*. 1964, **26**, 706.

[23] R.S.Nicholson, *Analytical Chemistry,* 1965, **37**, 1351.

[24] M Zhang,W.Han,M.Zhang,Y.Li,F.Zhu,Y.Xue,Chem. *Res. Chin. Univ.,* 2014, **30** , 489.

[25] H.Matsuda, Y. Z. Ayabe, *Z. Electrochem*., 1955, **59**, 494.

[25] S.Vandarkuzhali, N.Gogoi, S.Ghosh, N.Prabhakara Reddy, K.Nagarajan, *Electrochim.Acta.* 2012, **59**, 245.

[26] H. Tang, B. Pesic, *Electrochim. Acta,* 2014, **119**, 120.

Figure captions:

1. The schematic representation of the electrochemical set-up used in the cyclic votammetry measurement.

2. A Comparison of the cyclic voltammogram for pure LiCl-KCl melt and $CeCl_3$-LiCl-KCl melt in the potential range of 0 to -2.6V.Working electrode: molybdenum, $CeCl_3$:2.1×10^{-4}mol cm^{-3}, electrode area: 0.55cm^2, Temperature: 963 K, scan rate: 0.2 Vs^{-1}.

3. Energy dispersive X-ray fluorescence (EDXRF) spectra of the deposit (metallic cerium) obtained under potentiostatic condition in equimolar LiCl-KCl mixture at 963K (-2.05 V).

4. A Comparison of the cyclic voltammogram for pure NaCl-KCl melt and $CeCl_3$-NaCl-KCl melt in the potential range of 0 to -2.6V.Working electrode: Molybdenum, $CeCl_3$: 2.05×10^{-4}mol cm^{-3}, Electrode area: 0.38cm^2, Temperature: 963K, scan rate: 0.2Vs^{-1}.

5. SEM micrograph of the deposit product (metallic cerium) obtained under potentiostatic condition in equimolar LiCl-KCl mixture at 96K (-2.05 V).

6. Cyclic voltammogram for 2.1×10^{-4} molcm^{-3} of $CeCl_3$ in equimolar LiCl-KCl melt on molybdenum electrode at various scan rates. Electrode area: 0.53cm^2, Temperature: 963K.

7. Plot between the square root of scan rate and cathodic peak current for $CeCl_3$-LiCl-KCl melt. Concentration of $CeCl_3$:2.1×10^{-4}mol cm^{-3}, Electrode Area: 0.53cm^2, Temperature: 963K.

8. Cyclic voltammogram of $CeCl_3$-NaCl-KCl melt on molybdenum electrode at various scan rates.Concentration of $CeCl_3$:2.05×10^{-4} mol cm^{-3}, Electrode area: 0.38cm^2, Temperature: 963K.

9. Plot between the square root of scan rate and cathodic peak current for $CeCl_3$-NaCl-KCl melt. Concentration of $CeCl_3$:2.05×10^{-4}mol cm^{-3}, Electrode area: 0.38 cm^2, Temperature: 963K.

10. Square wave voltammogram for reduction of $CeCl_3$ at molybdenum electrode in LiCl-KCl melt. Experimental parameters are Pulseheight=25mv, Potentialstep=1mV, Frequency=5 kHz, $CeCl_3=2.05\times10^{-4}$ mol cm^{-3}, T = 963K

11. Net square wave voltammogram for reduction of $CeCl_3$ at molybdenum electrode in NaCl-KCl melt. Pulse height=25mv, Potential step=1mV, Frequency=5 kHz, $CeCl_3=2.0\times10^{-4}$mol cm^{-3}, T=963K.

12. Logarithm of the diffusion coefficient of Ce (III) as a function of inverse of temperature in (1) Equimolar LiCl-KCl melt (2) Equimolar NaCl-KCl melt.

13. Tafel for $CeCl_3$ in equimolar LiCl-KCl salt on Mo electrode $CeCl_3=2.1\times10^{-4}$ mol cm^{-3}, T = 963K Area of Mo=0.48cm^2,scan rate = 20 mV/s.

14. Tafel plot for $CeCl_3$ in equimolar NaCl-KCl salt on Mo electrode. $CeCl_3=2.0\times10^{-4}$ mol cm^{-3}, T = 963K Area of Mo=0.43cm^2, scan rate = 20 mV/s.

Table captions:

1. Rate constant (*Ks*) values obtained using Nicholson method.

2. Diffusion coefficient of Ce (III) evaluated from different cyclic voltammetry technique in equimolar LiCl-KCl and NaCl-KCl melt.

3. Variation of diffusion coefficient of Ce (III) with the temperature and activation energy of the diffusion process in equimolar LiCl-KCl and NaCl-KCl melts.

4. Evaluation of exchange current density on Mo and W at various temperatures in LiCl-KCl and NaCl-KCl .

Medium	$v/V.s^{-1}$	$\Delta E_P^T/V$	$\Delta E_P^{298}/V$	Ψ_{298}	Ψ_T	K_s
LiCl-KCl	0.05	0.132	0.12	0.356	0.639	9.0×10^{-3}
	0.1	0.165	0.15	0.212	0.380	7.56×10^{-3}
	0.15	0.216	0.18	0.15	0.269	6.56×10^{-3}
	0.2	0.231	0.21	0.1	0.179	5.04×10^{-3}
	0.3	0.243	0.225	-	-	-
	0.4	0.264	0.243	-	-	-
NaCl-KCl	0.05	0.198	0.183	0.15	0.328	4.03×10^{-3}
	0.075	0.210	0.194	0.125	0.224	3.37×10^{-3}
	0.1	0.225	0.208	0.1	0.179	3.11×10^{-3}
	0.15	0.280	0.259	-	-	-
	0.2	0.300	0.278	-	-	-
	0.3	0.320	0.296			

Table-1

Temperature	LiCl-KCl (10^5 D/cm^{2}s^{-1})		NaCl-KCl (10^5 D/cm^{2}s^{-1})	
	Mo	W	Mo	W
963	3.48 (±.02)	3.53 (±0.05)	2.65 (±0.03)	2.68 (±.01)
993	4.08 (±.04)	4.05 (±0.03)	3.09 (±0.01)	3.10 (±.01)
1023	4.49 (±.03)	4.45 (±0.06)	3.56 (±0.02)	3.54 (±.03)
1053	5.05 (±.05)	5.04 (±0.03)	4.08 (±0.02)	4.05 (±.02)

Table-2

Medium	Equation $\log D_{Ce(III)} = A + B/T$		$-\Delta H/kJmol^{-1}$
	A	B	
LiCl-KCl	-2.59	-1786	34.2
NaCl-KCl	-2.38	-2108	40.3

Tabl-3

Media	Temperature	J_0 on Mo (Acm^{-2})	J_0 on W(Acm^{-2})	Value of α
LiCl-KCl	963	0.058	0.056	0.48
	993	0.064	0.065	0.56
	1023	0.070	0.070	0.62
	1053	0.076	0.075	0.52
NaCl-KCl	963	0.059	0.060	0.50
	993	0.065	0.065	0.43
	1023	0.071	0.069	0.68
	1053	0.075	0.077	0.55

Table-4

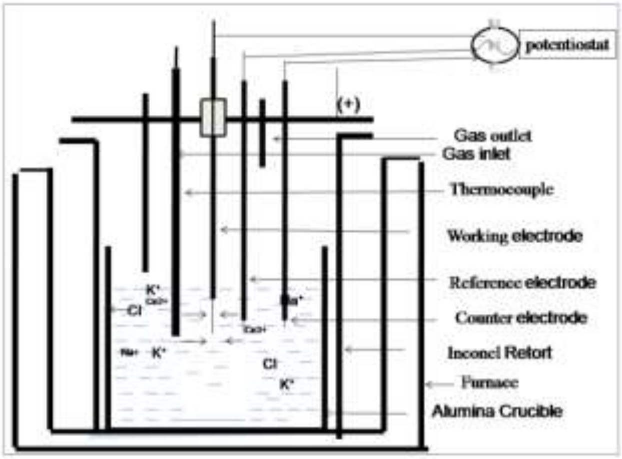
potentiostat
(+)
Gas outlet
Gas inlet
Thermocouple
Working electrode
Reference electrode
Counter electrode
Inconel Retort
Furnace
Alumina Crucible
K⁺
Cl
Na⁺
K⁺
Na⁺
Cl
K⁺

Fig.1

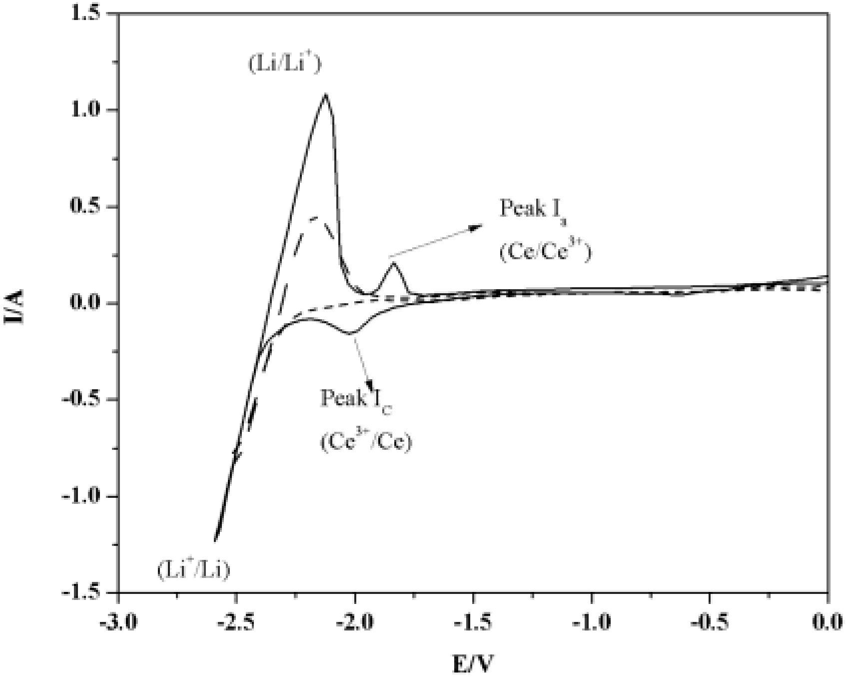
(Li/Li⁺)
Peak Ia
(Ce/Ce3+)
Peak IC
(Ce3+/Ce)
(Li⁺/Li)
I/A
E/V
1.5
1.0
0.5
0.0
-0.5
-1.0
-1.5
-3.0
-2.5
-2.0
-1.5
-1.0
-0.5
0.0

Fig.2

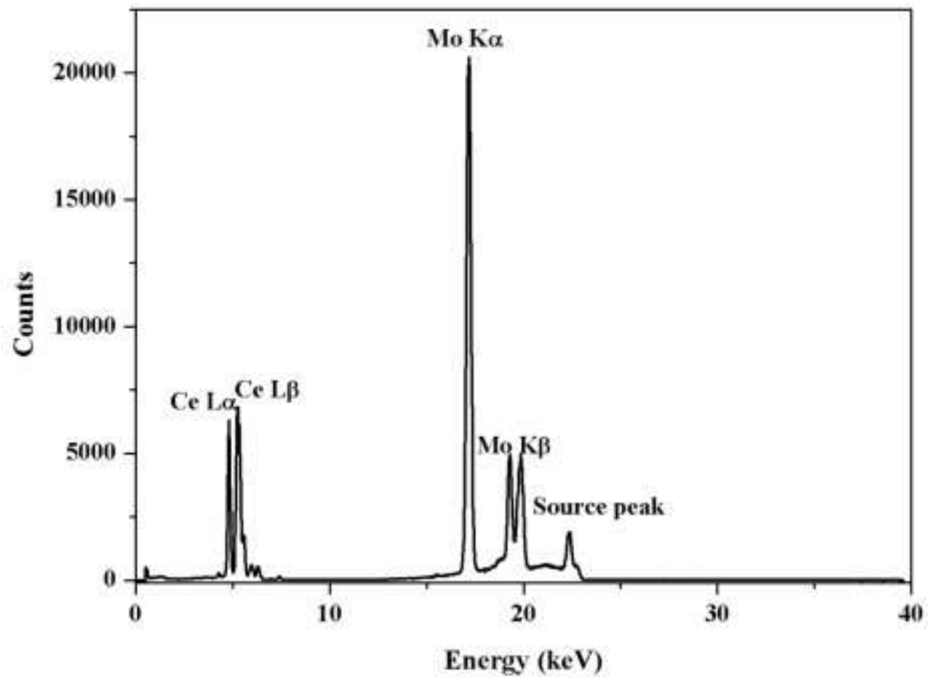
Mo Kα
Ce Lα
Ce Lβ
Mo Kβ
Source peak
Counts
0
5000
10000
15000
20000
0
10
20
30
40
Energy (keV)

Fig.3

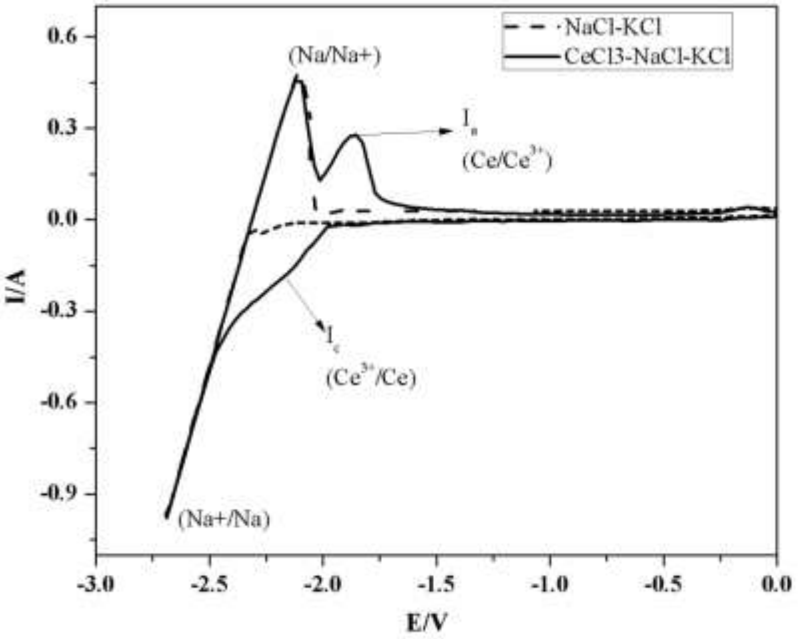
NaCl-KCl
CeCl3-NaCl-KCl
(Na/Na+)
I_a
(Ce/Ce^{3+})
I_c
(Ce^{3+}/Ce)
(Na+/Na)
0.6
0.3
0.0
-0.3
-0.6
-0.9
I/A
-3.0
-2.5
-2.0
-1.5
-1.0
-0.5
0.0
E/V

Fig.4

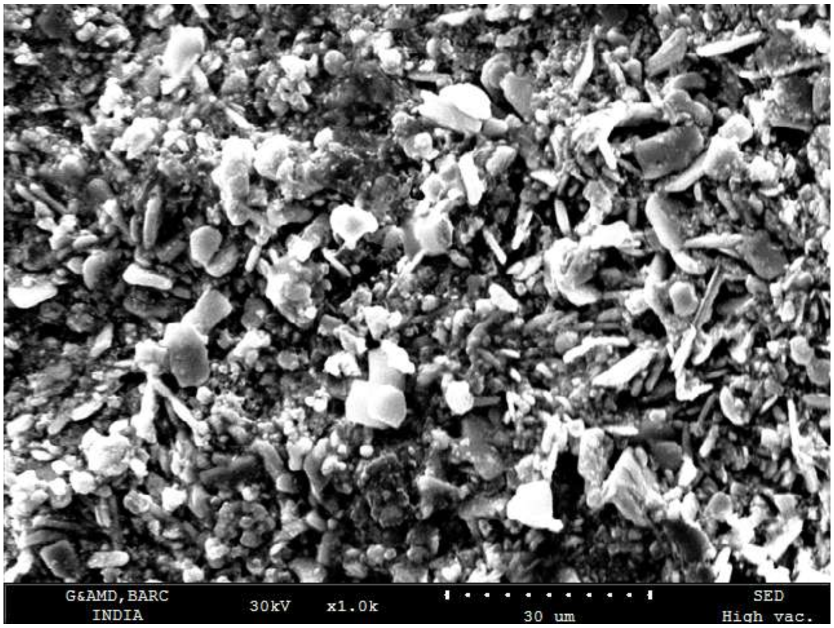
G&AMD,BARC
INDIA
30kV
x1.0k
30 um
SED
High vac.

Fig.5

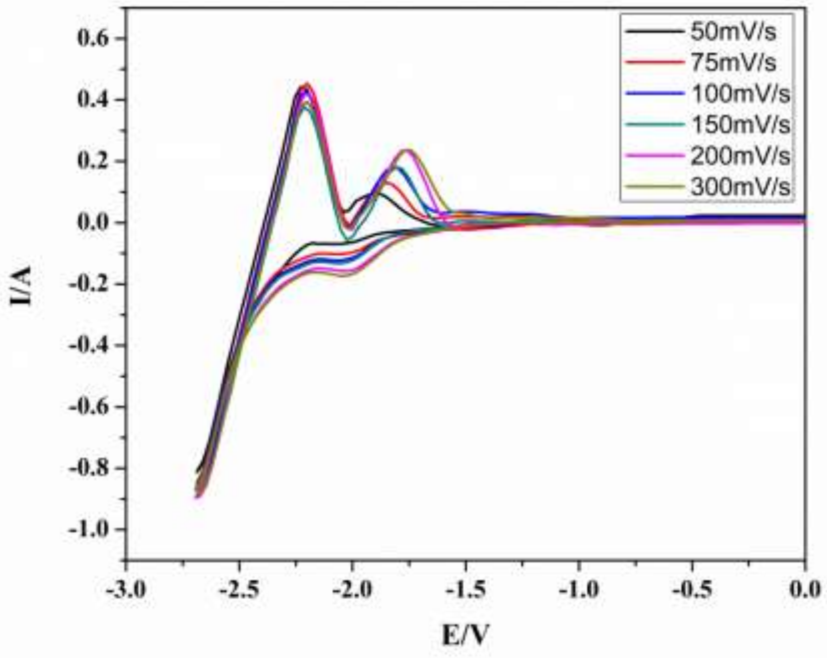
50mV/s
75mV/s
100mV/s
150mV/s
200mV/s
300mV/s
0.6
0.4
0.2
0.0
-0.2
-0.4
-0.6
-0.8
-1.0
I/A
-3.0
-2.5
-2.0
-1.5
-1.0
-0.5
0.0
E/V

Fig.6

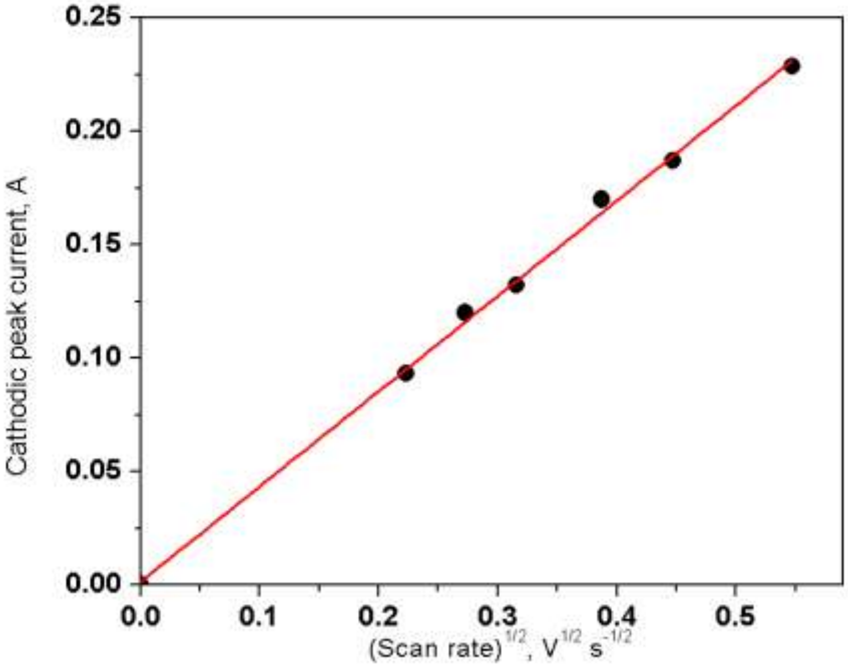
0.25
0.20
0.15
0.10
0.05
0.00
Cathodic peak current, A
0.0
0.1
0.2
0.3
0.4
0.5
(Scan rate)$^{1/2}$, V$^{1/2}$ s$^{-1/2}$

Fig.7

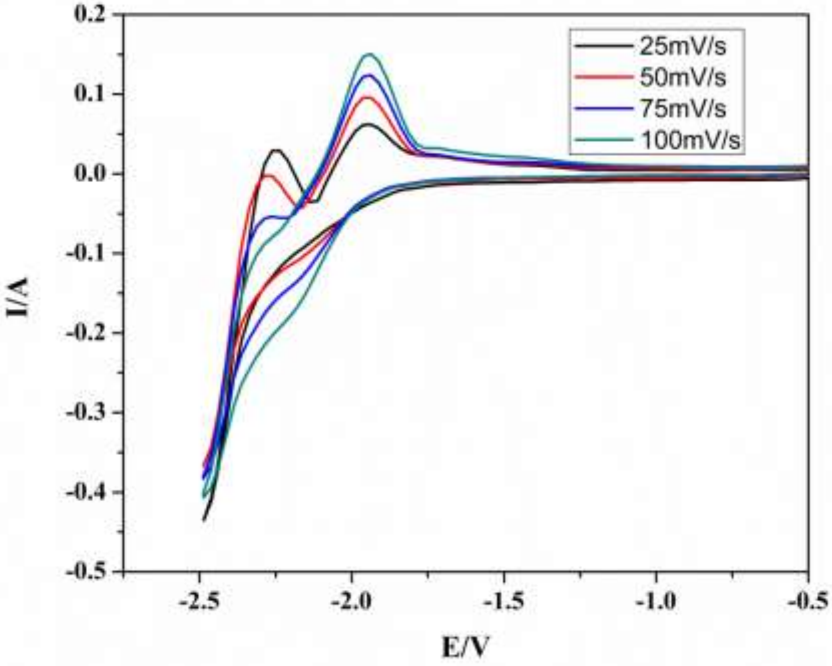
25mV/s
50mV/s
75mV/s
100mV/s
0.2
0.1
0.0
-0.1
-0.2
-0.3
-0.4
-0.5
I/A
-2.5
-2.0
-1.5
-1.0
-0.5
E/V

Fig.8

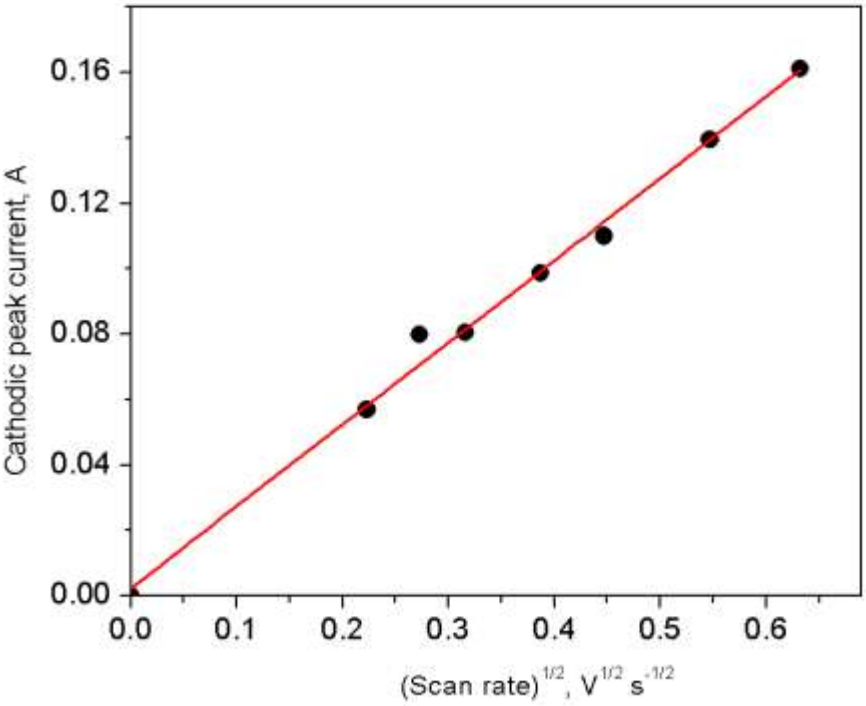
Cathodic peak current, A
0.00
0.04
0.08
0.12
0.16
0.0
0.1
0.2
0.3
0.4
0.5
0.6
(Scan rate)$^{1/2}$, V$^{1/2}$ s$^{-1/2}$

Fig.9

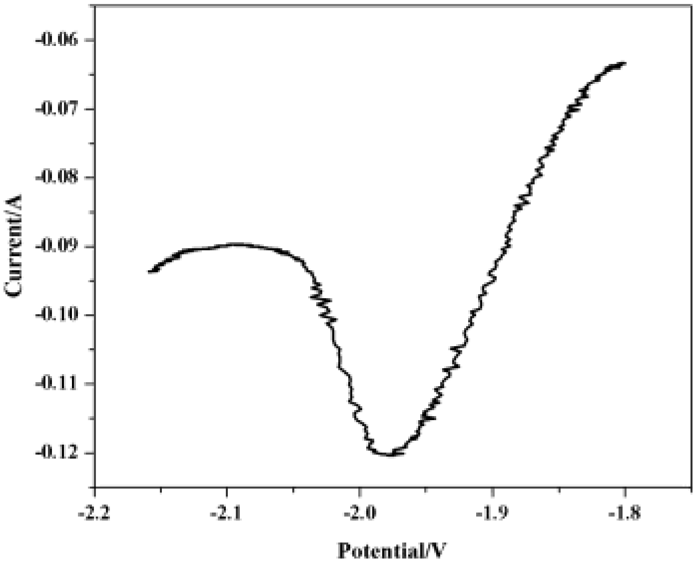
Current/A
-0.06
-0.07
-0.08
-0.09
-0.10
-0.11
-0.12
-2.2
-2.1
-2.0
-1.9
-1.8
Potential/V

Fig.10

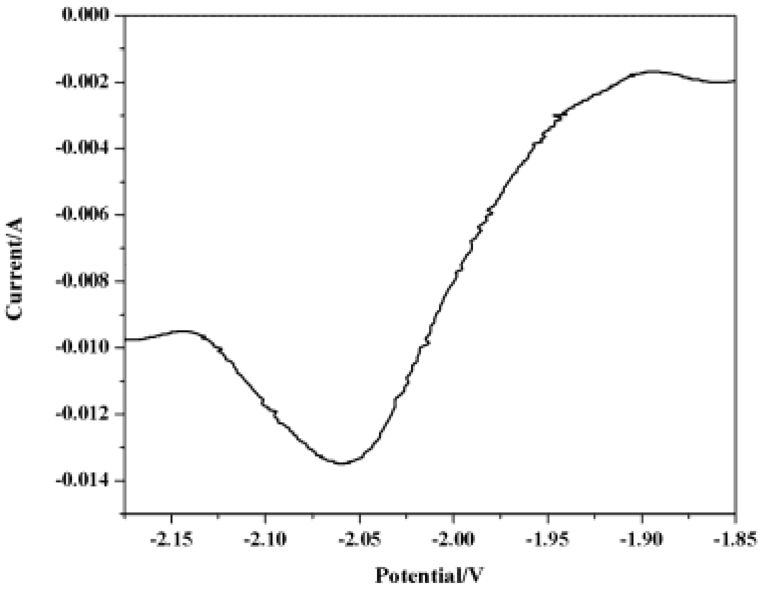
0.000
-0.002
-0.004
-0.006
-0.008
-0.010
-0.012
-0.014
Current/A
-2.15
-2.10
-2.05
-2.00
-1.95
-1.90
-1.85
Potential/V

Fig.11

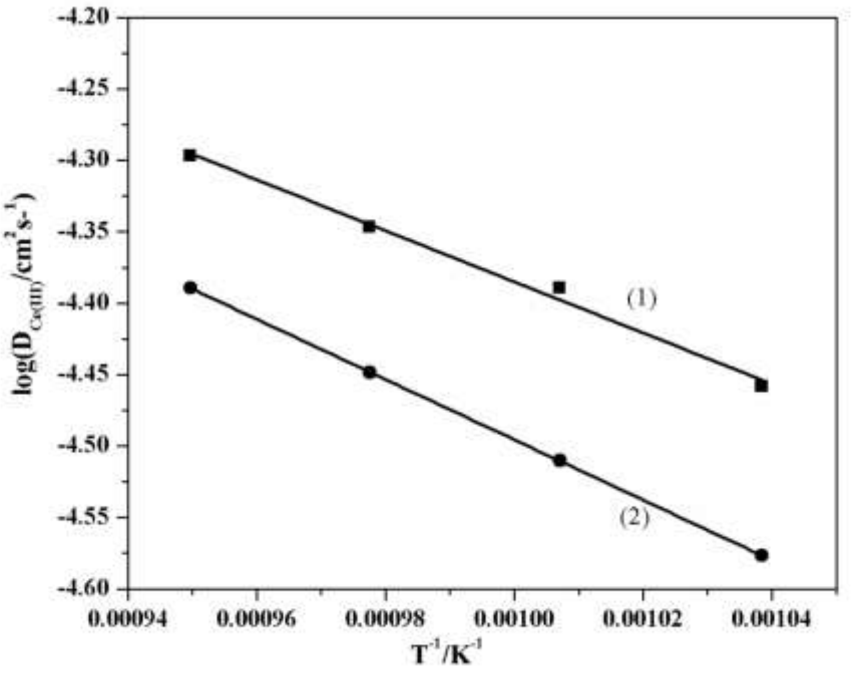
-4.20
-4.25
-4.30
-4.35
-4.40
-4.45
-4.50
-4.55
-4.60
log(D$_{Ce(III)}$/cm^{2}s^{-1})
(1)
(2)
0.00094
0.00096
0.00098
0.00100
0.00102
0.00104
T^{-1}/K^{-1}

Fig.12

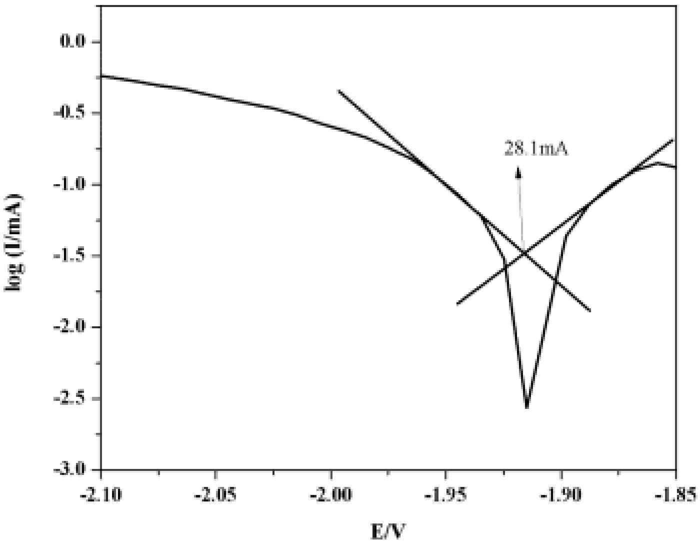
0.0
-0.5
-1.0
-1.5
-2.0
-2.5
-3.0
log (I/mA)
-2.10
-2.05
-2.00
-1.95
-1.90
-1.85
E/V
28.1mA

Fig. 13

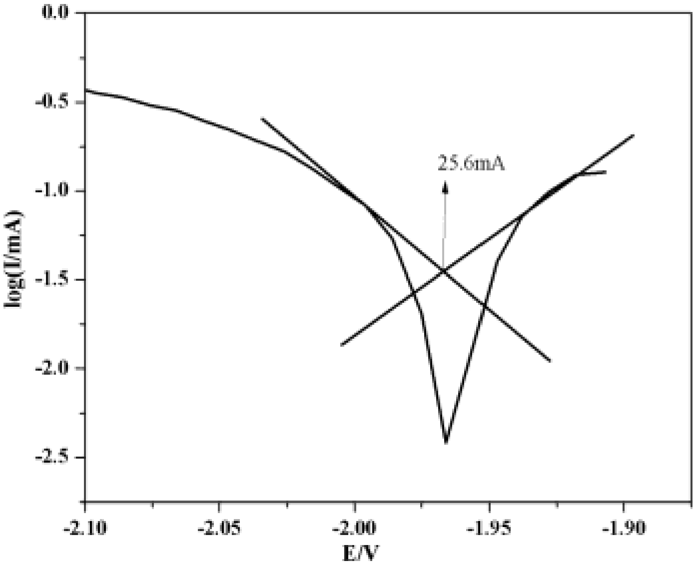
0.0
-0.5
-1.0
-1.5
-2.0
-2.5
log(I/mA)
-2.10
-2.05
-2.00
-1.95
-1.90
E/V
25.6mA

Fig.14